Photoelectron spectroscopy and *ab initio* study of the doubly antiaromatic B_6^{2-} dianion in the LiB_6^- cluster

Anastassia N. Alexandrova and Alexander I. Boldyrev[a)]
Department of Chemistry and Biochemistry, Utah State University, Logan, Utah 84322-0300

Hua-Jin Zhai and Lai-Sheng Wang[b)]
Department of Physics, Washington State University, Richland, Washington 99352 and W. R. Wiley Environmental Molecular Sciences Laboratory, Pacific Northwest National Laboratory, MS K8-88, Richland, Washington 99352

(Received 13 October 2004; accepted 3 November 2004; published online 20 January 2005)

A metal-boron mixed cluster LiB_6^- was produced and characterized by photoelectron spectroscopy and *ab initio* calculations. A number of electronic transitions were observed and used to compare with theoretical calculations. An extensive search for the global minimum of LiB_6^- was carried out via an *ab initio* genetic algorithm technique. The pyramidal $C_{2v}(^1A_1)$ molecule was found to be the most stable at all levels of theory. The nearest low-lying isomer was found to be a triplet $C_2(^3B)$ structure, 9.2 kcal/mol higher in energy. Comparison of calculated detachment transitions from LiB_6^- and the experimental photoelectron spectra confirmed the C_{2v} pyramidal global minimum structure. Natural population calculation revealed that LiB_6^- is a charge-transfer complex, $Li^+B_6^{2-}$, in which Li^+ and B_6^{2-} interact in a primarily ionic manner. Analyses of the molecular orbitals and chemical bonding of B_6^{2-} showed that the planar cluster is twofold (π- and σ-) antiaromatic, which can be viewed as the fusion of two aromatic B_3^- units. © *2005 American Institute of Physics.* [DOI: 10.1063/1.1839575]

I. INTRODUCTION

Boron is an intriguing element with unique properties. It has a vast chemistry,[1,2] second only probably to its neighbor, carbon. The majority of boron compounds contain three-dimensional cage structures. However, extensive computational studies in the past two decades predicted a highly unusual planar or quasiplanar world for elemental boron clusters.[3–29] Surprisingly, relatively scare experimental attention was paid to boron clusters. Most of the previous experimental studies on boron clusters[4,30–38] were mass spectrometry based, revealing little direct structural or electronic information. Recently, in an effort to elucidate the structure and bonding of small boron clusters, we published a series of joint photoelectron spectroscopic and theoretical studies on small boron clusters, B_n^- and B_n from $n=3-15$.[39–44] We confirmed the planar or quasiplanar ground state structures for all these clusters. We further showed that both σ- and π-aromaticity and antiaromaticity are responsible for the unique planar shapes of these boron clusters.

The elucidation of chemical bonding in boron clusters opens an opportunity to design planar boron clusters as new inorganic ligands. In order for a bare boron cluster to be a potential ligand or building block of a solid material, it should acquire a closed shell electronic configuration. The reason for this requirement could be understood using aromatic hydrocarbons as an example. The cyclopentadiene C_5H_5 moiety need to acquire one more electron to form the stable closed-shell $C_5H_5^-$ anion, which is an important ligand in chemistry. The stability of the $C_5H_5^-$ anion derives from its (π)-aromaticity, analogous to benzene. As discussed in our previous papers,[39–46] boron clusters can possess multiple aromaticity (σ- and π-) due to strong delocalization of both σ and π electrons. Kuznetsov and Boldyrev have computationally studied the charge-transfer complexes, $M^+X_3^-$ (M = Li–Cs, X = B–Tl),[45] which contain the doubly aromatic X_3^- unit.[39] MB_6-type (M = Be–Ca) charge-transfer complexes have also been studied theoretically.[47] In a very recent photoelectron spectroscopy (PES) and *ab initio* study,[46] we showed how the doubly aromatic closed-shell B_8^{2-} molecular wheel can be used as an inorganic ligand in LiB_8^- and retains its σ- and π-aromatic characters in the charge-transfer complex.

In a previous study on the boron hexamer,[41] we showed that B_6 possesses a planar structure with a triplet group state. We further showed computationally that the B_6^{2-} doubly charged anion is closed shell, but is antiaromatic. Thus, B_6^{2-} is not D_{6h}, rather it possesses a lower symmetry D_{2h} structure. In this paper, we present a joint theoretical and experimental study of the LiB_6^- cluster, which contains the antiaromatic B_6^{2-} structural unit. The LiB_6^- cluster was produced by laser vaporization and characterized using PES. Six electronic transitions were observed. An extensive search for the global minimum of LiB_6^- was performed via an *ab initio* genetic algorithm technique. A pyramidal $C_{2v}(^1A_1)$ molecule was found to be the most stable at all levels of theory. The second low-lying isomer was found to be a triplet $C_2(^3B)$ structure. Comparisons of the calculated electronic transitions and experimental photoelectron spectra showed distinctly the presence of the pyramidal species in the cluster

a)Electronic mail: boldyrev@cc.usu.edu
b)Electronic mail: ls.wang@pnl.gov

beam. We showed by natural population analysis that LiB_6^- is indeed a charge-transfer complex, $Li^+B_6^{2-}$, in which the interaction between Li^+ and B_6^{2-} is primarily ionic. We further carried out a detailed analysis of the chemical bonding in the B_6^{2-} unit and proved that it is indeed doubly antiaromatic (both σ- and π-) and can be viewed as the fusion of two aromatic B_3^-.

II. EXPERIMENTAL METHOD

The experiment was carried out using a magnetic-bottle time-of-flight PES apparatus equipped with a laser vaporization supersonic cluster source.[48,49] Briefly, lithium-boron mixed cluster anions were produced by laser vaporization of a B/Li mixed target in the presence of a helium carrier gas. The target contained ~30% Li in molar ratio and was 99.75% ^{10}B enriched. Various B_n^- and LiB_n^- clusters were produced from the cluster source, and were analyzed using a time-of-flight mass spectrometer. The LiB_6^- anions with a mass/charge ratio of 67 were mass selected and decelerated before being photodetached. The use of ^{10}B isotope-enriched boron greatly simplified the mass analysis and allowed a clean mass selection. Three detachment photon energies were used in the current experiment: 355 nm (3.496 eV), 266 nm (4.661 eV), and 193 nm (6.424 eV). Photoelectrons were collected at nearly 100% efficiency by a magnetic bottle and analyzed in a 3.5 m long electron flight tube. Photoelectron spectra were calibrated using the known spectrum of Rh^-, and the resolution of the apparatus was $\Delta Ek/Ek \sim 2.5\%$, that is, ~25 meV for 1 eV electrons.

III. THEORETICAL METHODS

Initial search for the global minima of the LiB_6^- cluster was performed using the *ab initio* gradient embedded genetic algorithm (GEGA) program.[50,51] The hybrid method, known as B3LYP,[52–54] with relatively small basis set 3-21G was employed throughout the execution of the GEGA. Briefly, within the GEGA procedure, the initial geometries of individuals in the population are randomly generated and further optimized to the nearest local minima on the potential energy surface, using the GAUSSIAN 03 package.[55] If a saddle point is encountered the normal mode of the first imaginary frequency is followed until a local minimum is found. Further, the population, composed of the thus selected good individuals, undergoes breeding and mutations. The mating, implemented in GEGA, is performed based on the robust technique originally proposed in 1995 by Deaven and Ho.[56] Probabilities to be breed are assigned according to the best-fit (lowest-energy) criterion. Based on the probabilities, couples of parents are randomly selected. The geometries of parents are cut by a random cutting plane, and the thus obtained halves (genes) are then recombined either in a simple or in a head-to-tail manner to form a new cluster (child). The number of atoms in the newly generated geometry is checked, and the new cluster is optimized to the nearest local minimum. After the number of individuals in the population is doubled within the breeding process, the best-fit group is selected and convergence of the algorithm is checked. The GEGA is considered converged if the current lowest-energy species (global minimum or at least very stable local minimum) remains for 20 iterations. If the convergence is not yet met, the highest energy species in the population undergo mutations with a mutation rate set to 33.33%. Mutations involve displacements of random atoms of a cluster in arbitrary directions, with the purpose of changing the initial geometry so as to push the structure out of the current local minimum to another well on the potential energy surface. Mutants are optimized to the nearest local minima. After that the algorithm proceeds with the new cycle of breeding. All low-lying isomers are detected and stored throughout the execution and they are reported to the user at the end of the run. A few runs of GEGA are done on the system in order to confirm the found global minimum structure.

The geometry and vibrational frequencies of the thus identified global minimum, as well as low-lying isomers, were further refined at higher levels of theory. The B3LYP and the coupled-cluster [CCSD(T)] (Refs. 57–59) methods with polarized split-valence basis sets (6-311+G*) (Refs. 60 and 61) were used for this purpose. CASSCF(8,8)/6-311+G* calculations were performed for the global minimum structure in order to test the applicability of the other theoretical methods based on the one-electron approximation. Natural population analysis[62] was carried out to assess the charge distribution. Vertical electron detachment energies (VDEs) were calculated using the restricted and unrestricted coupled-cluster methods U(R)CCSD(T)/6-311++G(2*df*), the time-dependent density functional methods TD-B3LYP/6-311+G(2*df*),[63–65] and the outervalence Green-function method R(U)OVGF/6-311+G(2*df*).[66–69] Molecular orbitals (MOs) were calculated at the HF/6-311+G* level of theory. B3LYP, U(R)CCSD(T), HF, and TD-B3LYP calculations were performed using GAUSSIAN 03. The R(U)OVGF calculations were done using the GAUSSIAN 98 program.[70] Molecular orbitals were made using the MOLDEN 3.4 program.[71]

IV. EXPERIMENTAL RESULTS

The photoelectron spectra of LiB_6^- are shown in Fig. 1 at three photon energies. The 355 nm spectrum revealed two rather diffused bands (*X* and *A*). The ground state transition (*X*) yielded a VDE of 2.60±0.03 eV from the peak maximum. Since no vibrational structures were resolved, the adiabatic detachment energy (ADE) was evaluated from the onset of band *X* by drawing a straight line at the leading edge of the band and then adding the instrumental resolution to the intersection with the binding energy axis. The ADE thus evaluated was 2.3±0.1 eV, which also represents the electron affinity of the LiB_6 neutral. Because of the broad spectral feature, a large uncertainty was assessed for the obtained electron affinity. The extended tail (~1.8–2.2 eV) at the lower binding energy side of band *X* is assigned to hot band transitions, with possible contributions from other minor isomers, as will be discussed below. Band *A* appeared as a shoulder of band *X* in the 355 nm spectrum, but became better defined in the 266 and 193 nm spectra. The VDE of band *A* was estimated to be 2.97 eV. Four more bands were observed in the higher photon energy spectra with VDEs: *B*

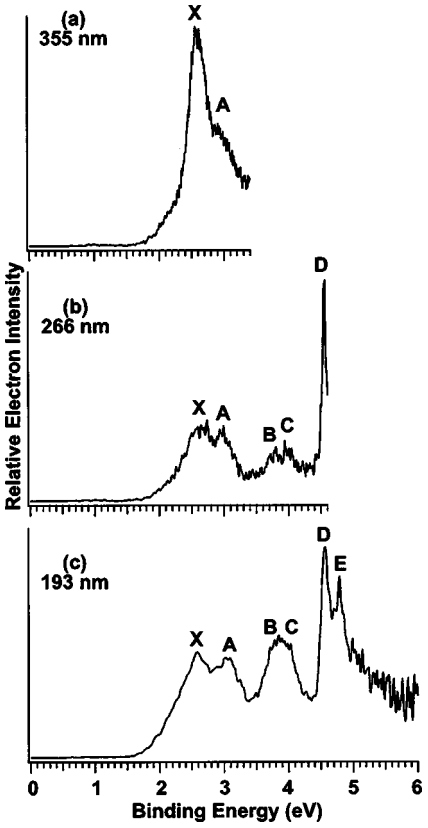

FIG. 1. Photoelectron spectra of LiB_6^- at (a) 355 nm (3.496 eV), (b) 266 nm (4.661 eV), and (c) 193 nm (6.424 eV).

(3.76 eV), *C* (4.00 eV), *D* (4.56 eV), and *E* (4.79 eV). Bands *B* and *C* were also very broad, whereas bands *D* and *E* were intense and sharp. Overall, six detachment transitions were resolved for LiB_6^-, which will serve as electronic ''fingerprints'' of the complex for comparison with theory (see below). All obtained VDEs are collected in Table I.

V. THEORETICAL RESULTS

The computational search for the global minimum of LiB_6^- revealed the pyramidal structure I, $C_{2v}(^1A_1)$ (Fig. 2). Natural population analysis showed that the chemical bonding between Li^+ and B_6^{2-} fragments is primarily ionic: $Q(\mathrm{Li}) = +0.88|e|$ (B3LYP/6-311+G*). The pyramidal species with the Li^+ cation coordinated to the almost planar B_6^{2-} dianion is reminiscent of the global minimum structure previously found for B_6^{2-} (a distorted hexagonal D_{2h} structure).[41] The electronic configuration of this species is $1a_1^2 1b_2^2 1b_1^2 2a_1^2 3a_1^2 1a_2^2 4a_1^2 2b_1^2 2b_2^2 3b_2^2$. The second low-energy isomer II (Fig. 2) has a pyramidal triplet structure $C_2(^3\mathrm{B})$ with Li^+ above a distorted $C_{2h}\,B_6^{2-}$. It was found to

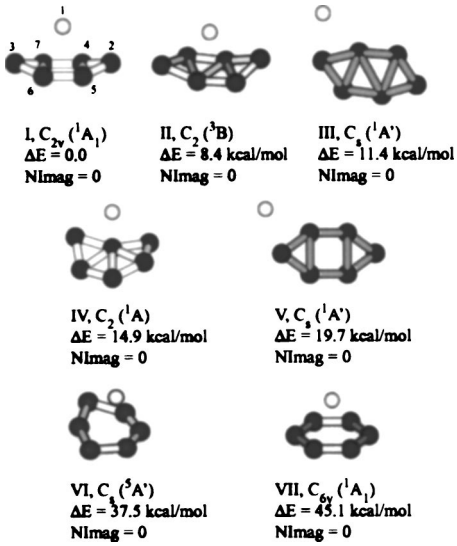

FIG. 2. Low-lying isomers of LiB_6^- and their relative energies at the B3LYP/6-311+G* level of theory.

be 9.2 kcal/mol [CCSD(T)/6-311+G(2*df*)//B3LYP/6-311+G*] higher in energy than the global minimum. The lowest singlet planar $C_s(^1A')$, structure III in Fig. 2, is 14.1 kcal/mol [CCSD(T)/6-311+G(2*df*)//B3LYP/6-311+G*] above the global minimum. Calculated geometries and harmonic frequencies of the global minimum structure at three levels of theory are collected in Table II. As one can see the computational results agree rather well at all three levels of theory. The Hartree–Fock wave function was found to be dominant ($C_{\mathrm{HF}} = 0.91$) in the CASSCF(8,8)/6-311+G* calculations, thus justifying the use of the B3LYP/6-311+G* and CCSD(T)/6-311+G* methods. All low-lying isomers of LiB_6^-, found within 20 kcal/mol above the global minimum, with an addition of the quintet structure VI are shown in Fig. 2, whereas the calculated properties of selected low-lying isomers were collected in Table III. In the recent computational study,[46] BeB_6 and MgB_6 were proposed to have C_{6v} ground states, which each contains a hexagonal $D_{6h}\,B_6^{2-}$. Our data showed that an analogous structure for LiB_6^- (structure VII in Fig. 2) is 45.1 kcal/mol (B3LYP/6-311+G*) less stable than the ground state $C_{2v}(^1A_1)$ structure.

VI. INTERPRETATION OF PHOTOELECTRON SPECTRA

In order to verify the global minimum structure of LiB_6^-, we compared the *ab initio* photoelectron spectra obtained using several theoretical methods (Table IV) with the experimental data (Table I and Fig. 1). At all employed levels of theory, we found that the feature *X* of the experimental

TABLE I. Observed vertical detachment energies (VDEs) from the photoelectron spectra of LiB_6^-.

	X[a]	*A*	*B*	*C*	*D*	*E*
VDE (eV)[b]	2.60 (3)	2.97 (3)	3.76 (5)	4.00 (5)	4.56 (2)	4.79 (3)

[a]The adiabatic detachment energy (ADE) was evaluated to be 2.3±0.1 eV, which also represents the electron affinity of the LiB_6 neutral.
[b]Numbers in the parentheses indicate the experimental uncertainties in the last digit.

TABLE II. Calculated molecular properties of the global minimum structure I of LiB_6, C_{2v} ($^1A_1$).

Method		B3LYP/6-311+G*				CCSD(T)/6-311+G*				CASSCF(8,8)/6-311+G*		
E_{total} (a.u.)		−156.501 219				−155.962 144[a]				−155.416 440[b]		
Geometry (Å)	Li	0.0000	0.0000	1.6420	Li	0.0000	0.0000	1.6609	Li	0.0000	0.0000	1.6931
	B	0.0000	2.0209	0.0391	B	0.0000	2.0637	0.0438	B	0.0000	2.0527	0.0279
	B	0.0000	−2.0209	0.0391	B	0.0000	−2.0637	0.0438	B	0.0000	−2.0527	0.0279
	B	0.8932	0.8313	−0.2658	B	0.9058	0.8406	−0.2710	B	0.8869	0.8342	−0.2679
	B	−0.8932	0.8313	−0.2658	B	−0.9058	0.8406	−0.2710	B	−0.8869	0.8342	−0.2679
	B	−0.8932	−0.8313	−0.2658	B	−0.9058	−0.8406	−0.2710	B	−0.8869	−0.8342	−0.2679
	B	0.8932	−0.8313	−0.2658	B	0.9058	−0.8406	−0.2710	B	0.8869	−0.8342	−0.2679
$\omega_1(a_1)$ (cm^{-1})		1320 (6.8)[c]				1238				1294		
$\omega_2(a_1)$ (cm^{-1})		795 (0.0)				775				829		
$\omega_3(a_1)$ (cm^{-1})		627 (2.1)				617				676		
$\omega_4(a_1)$ (cm^{-1})		500 (80.6)				493				497		
$\omega_5(a_1)$ (cm^{-1})		226 (22.8)				206				249		
$\omega_6(a_2)$ (cm^{-1})		1108 (0.0)				1030				1037		
$\omega_7(a_2)$ (cm^{-1})		499 (0.0)				470				536		
$\omega_8(a_2)$ (cm^{-1})		281 (0.0)				228				237		
$\omega_9(b_1)$ (cm^{-1})		1289 (0.0)				1232				1258		
$\omega_{10}(b_1)$ (cm^{-1})		642 (0.6)				610				656		
$\omega_{11}(b_1)$ (cm^{-1})		245 (14.9)				248				298		
$\omega_{12}(b_2)$ (cm^{-1})		1251 (311.1)				1188				1255		
$\omega_{13}(b_2)$ (cm^{-1})		680 (66.5)				657				742		
$\omega_{14}(b_2)$ (cm^{-1})		460 (1.1)				432				497		
$\omega_{15}(b_2)$ (cm^{-1})		153 (20.2)				174				170		

[a]At the CCSD(T)/6-311+G(2*df*)/CCSD(T)/6-311+G* level of theory $E_{total}=-156.033\,178$ a.u.
[b]$C_{HF}=0.91$.
[c]Infrared intensities are shown in parentheses.

spectrum with a VDE of 2.60 eV can clearly be assigned to the detachment of an electron from the highest occupied molecular orbital (HOMO) ($3b_2$) of the lowest-energy C_{2v} structure I. The $3b_2$ HOMO (Fig. 3) is a σ-type orbital with partial bonding character among two B_3 units involving atoms 2-4-5 and 3-6-7 (Fig. 2). The broad spectral feature suggested a significant geometry change upon the electron detachment, consistent with the bonding nature of the

TABLE III. Calculated molecular properties of low-lying isomers II, III, and IV of LiB_6^- at the B3LYP/6-311+G* level of theory.

Isomers		II, C_2 (^{3}B)				III, C_s ($^1A'$)				IV, C_2 (^1A)		
E_{total} (a.u.)		−156.487 784[a]				−156.483 014[b]				−156.477 432		
Geometry (Å)	Li	0.0000	0.0000	1.6708	B	1.4219	−0.0993	0.0000	Li	0.0000	0.0000	−2.3123
	B	0.0000	2.0431	0.1250	B	1.6306	−1.5817	0.0000	B	0.0000	0.0000	−0.2361
	B	0.0000	−2.0431	0.1250	B	0.1195	−1.3316	0.0000	B	0.0000	1.6367	−0.7049
	B	1.0137	0.9631	−0.2818	B	−1.2654	−0.4461	0.0000	B	0.0000	−1.6367	−0.7049
	B	−0.6442	0.6130	−0.3444	B	−1.5544	1.0395	0.0000	B	−0.4100	1.3503	0.7750
	B	−1.0137	−0.9631	−0.2818	B	0.0000	0.6977	0.0000	B	0.4100	−1.3503	0.7750
	B	0.6442	−0.6130	−0.3444	Li	−0.5869	2.8691	0.0000	B	0.0000	0.0000	1.4832
Frequencies (cm^{-1})		$\omega_1(a)=1269$ (6.2)[c]				$\omega_1(a')=1303$ (34.1)[c]				$\omega_1(a)=1030$ (173.6)[c]		
		$\omega_2(a)=935$ (0.1)				$\omega_2(a')=1340$ (48.4)				$\omega_2(a)=945$ (0.3)		
		$\omega_3(a)=850$ (1.9)				$\omega_3(a')=1230$ (362.9)				$\omega_3(a)=712$ (5.4)		
		$\omega_4(a)=638$ (15.5)				$\omega_4(a')=1060$ (54.9)				$\omega_4(a)=584$ (10.3)		
		$\omega_5(a)=576$ (3.5)				$\omega_5(a')=846$ (20.5)				$\omega_5(a)=540$ (0.0)		
		$\omega_6(a)=516$ (36.8)				$\omega_6(a')=715$ (49.8)				$\omega_6(a)=467$ (82.7)		
		$\omega_7(a)=412$ (7.1)				$\omega_7(a')=672$ (2.2)				$\omega_7(a)=227$ (70.1)		
		$\omega_8(a)=175$ (40.4)				$\omega_8(a')=572$ (32.1)				$\omega_8(b)=1248$ (11.9)		
		$\omega_9(b)=1162$ (70.0)				$\omega_9(a')=537$ (54.2)				$\omega_9(b)=1036$ (32.4)		
		$\omega_{10}(b)=1087$ (0.1)				$\omega_{10}(a')=285$ (36.6)				$\omega_{10}(b)=835$ (4.5)		
		$\omega_{11}(b)=751$ (63.7)				$\omega_{11}(a')=111$ (76.1)				$\omega_{11}(b)=554$ (27.3)		
		$\omega_{12}(b)=546$ (5.6)				$\omega_{12}(a'')=440$ (0.4)				$\omega_{12}(b)=395$ (10.5)		
		$\omega_{13}(b)=478$ (0.2)				$\omega_{13}(a'')=274$ (1.4)				$\omega_{13}(b)=298$ (36.5)		
		$\omega_{14}(b)=196$ (16.2)				$\omega_{14}(a'')=183$ (0.3)				$\omega_{14}(b)=280$ (0.4)		
		$\omega_{15}(b)=170$ (10.6)				$\omega_{15}(a'')=32$ (48.4)				$\omega_{15}(b)=163$ (37.2)		

[a]At the CCSD(T)/6-311+G(2*df*)/B3LYP/6-311+G* level of theory $E_{total}=-156.018\,547$ a.u.
[b]At the CCSD(T)/6-311+G(2*df*)/B3LYP/6-311+G* level of theory $E_{total}=-156.010\,679$ a.u.
[c]Infrared intensities are shown in parentheses.

TABLE IV. Calculated vertical detachment energies (VDEs) of global minimum structure I of LiB_6^-, and the low-lying isomers II, III, and IV.

Structure	Molecular orbital	VDE_{theor} eV ROVGF/6-311+G(2df)[a]	TD B3LYP/6-311+G(2df)	RCCSD(T)/6-311+G(2df)
I, $C_{2v}(^1A_1)$	$3b_2$	2.57 (0.86)	2.36	2.71
	$2b_2$	3.12 (0.87)	3.06	
	$2b_1$	3.78 (0.86)	3.92	3.68
	$4a_1$	4.18 (0.82)	4.04	4.08
	$1a_2$	5.41 (0.85)	5.21	5.22
II, $C_2(^3B)$	$6a, \alpha$	2.31 (0.90)[b]	2.21	
	$4b, \beta$	2.47 (0.90)	2.66	
	$5b, \alpha$		2.79	
	$4b, \alpha$		3.14	
	$5a, \beta$	3.55 (0.90)	3.72	
	$3b, \beta$	3.70 (0.88)	3.91	
	$3b, \alpha$		4.16	
	$5a, \alpha$		4.21	
	$4a, \alpha$		4.44	
	$4a, \beta$	4.45 (0.87)	4.55	
	$3a, \beta$	5.58 (0.85)	5.29	
	$3a, \alpha$		5.89	
III, $C_s(^1A')$	$2a''$	2.09 (0.87)	1.95	
	$8a'$	2.57 (0.86)	2.53	
	$7a'$	3.92 (0.83)	3.68	
	$6a'$	3.85 (0.85)	4.07	
	$1a''$	4.58 (0.80)	4.21	
	$5a'$	5.14 (0.81)	4.96	
IV, $C_2(^1A)$	$5a$	2.10 (0.87)	2.00	
	$5b$	2.97 (0.84)	2.86	
	$4b$	4.03 (0.85)	3.73	
	$4a$	4.95 (0.83)	4.76	
	$3b$	5.53 (0.84)	5.16	

[a]Numbers in parentheses represent pole strength.
[b]Calculation done at the UOVGF/6-311+G(2*d*) level.

HOMO. Peak *A* of the PES spectrum with a VDE of 2.97 eV corresponds well to the calculated VDE for detachment from the HOMO-1 ($2b_2$), which is a partially bonding orbital with π-character. Features *B* (VDE: 3.76 eV) and *C* (VDE: 4.00 eV) can be assigned to electron detachments from the HOMO-2 ($2b_1$) and HOMO-3 ($4a_1$), respectively. All these assignments are rather straightforward, and excellent agreement was observed between theory and experiment for all these transitions (*X*,*A*,*B*,*C*).

However, the higher binding energy feature *D*, observed at a VDE of 4.56 eV did not seem to agree well with the calculated higher detachment channel, i.e., HOMO-4 ($1a_2$). This was most likely due to the fact that the methods based on the one-electron approximation used in this work deteriorate at high binding energies and cause the large discrepancy with the experiment. In fact, we found that none of the methods worked for calculating the next detachment channel from HOMO-5 ($3a_1$), corresponding to the observed feature *E* at a VDE of 4.79 eV. Thus we conclude that the overall agreement between the calculated VDEs and the PES data are gratifying, landing credence to the C_{2v} global minimum structure I for LiB_6^-. The observed PES spectra also indicated that there might also be contributions from other low-lying isomers (e.g., isomers II, III, and IV), which all have lower electron binding energies. In particular, the weak tail between ~2.0 and 2.2 eV might come from the low lying isomers.

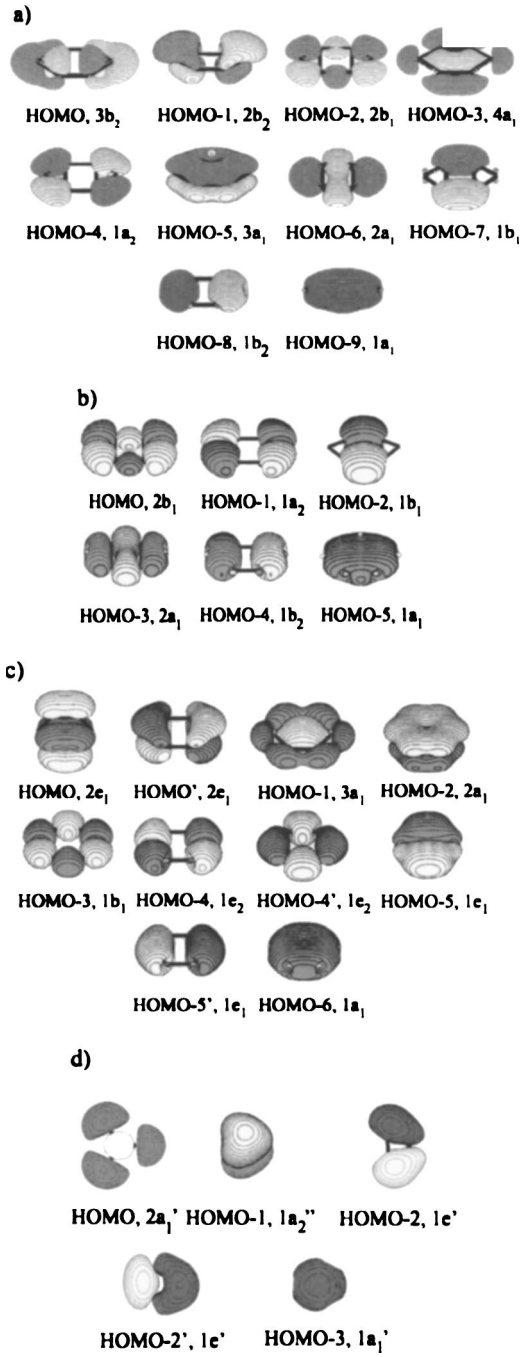

FIG. 3. Molecular orbital pictures of (a) the $C_{2v}(^1A_1)$ global minimum structure of LiB_6^-, (b) the LiB_6^{7+} model cluster at the geometry of the $C_{2v}(^1A_1)$ global minimum structure of LiB_6^-, (c) the $C_{6v}(^1A_1)$ isomer of LiB_6^-, and (d) the B_3^- cluster.

VII. CHEMICAL BONDING IN LiB_6^-

The isolated B_6^{2-} dianion has been studied by several group previously.[27,29,41] In all these studies the B_6^{2-} dianion was found to be a planar D_{2h} structure. Chemical bonding in this structure was characterized first by Fowler and co-

workers using maps of total, σ-only, and π-only current density. They concluded that the B_6^{2-} ring supports a paratropic π-current, and thus it is a π-antiaromatic system in accordance with the presence of 4π-electrons.

All valence MOs of the LiB_6^- anion are presented in Fig. 3(a). It shows that the presence of Li^+ only slightly affects the MOs of B_6^{2-}, confirming the primarily ionic character of the bonding in LiB_6^- ($Li^+B_6^{2-}$). Out of the ten valence orbitals, six are responsible for peripheral B–B bonding: HOMO-9 ($1a_1$), HOMO-8 ($1b_2$), HOMO-7 ($1b_1$), HOMO-6 ($2a_1$), HOMO-4 ($1a_2$), and HOMO-2 ($2b_1$). In order to prove that, we calculated a LiB_6^{7+} model cluster at the LiB_6^- geometry with occupation of only those six orbitals, which are presented in Fig. 3(b). We were able to localize these six delocalized MOs into six $2c-2e$ bonds corresponding to six peripheral B–B bonds with the occupation number of about 1.92. Thus, we identified six MOs, which are responsible exclusively for the peripheral bonding of the B_6^{2-} unit in LiB_6^-. The remaining four MOs correspond to bonding between boron atoms through the center of the cluster. Two of these orbitals, HOMO-5 ($3a_1$) and HOMO-1 ($2b_2$), are π-orbitals and the other two, HOMO-3 ($4a_1$) and HOMO ($3b_2$), are σ-orbitals [Fig. 3(a)]. The HOMO-5 is a completely bonding π-MO, and the HOMO-1 is a partially bonding π-MO, which originates from the degenerate π-MO pair $2e_1$ (HOMO) of the perfect hexagonal C_{6v} structure [Fig. 3(c)]. The occupation of only one degenerate $2e_1$-MO leads to the Jahn-Teller distortion to the C_{2v} structure of LiB_6^-, which is thus π-antiaromatic. The HOMO-3 is a completely bonding σ-MO, similar to the completely bonding HOMO-5 π-MO. The HOMO is a partially bonding σ-MO, which originates from the degenerate σ-MO $3e_1$ lowest unoccupied molecular orbital (LUMO) of the C_{6v} hexagonal structure. The partial occupation of this degenerate e_1-MO also leads to the Jahn-Teller distortion to the C_{2v} structure for LiB_6^- and makes it σ-antiaromtic. Thus both the π- and σ-Jahn-Teller distortions are enforcing the C_{2v} geometry on the LiB_6^- anion. We recently proved that when two π-electrons are removed from the B_6^{2-} dianion the resulting neutral B_6 cluster becomes π-aromatic with two π electrons. But B_6 is still distorted from the perfect hexagon structure, because it is σ-antiaromatic.[41] From the MO analysis, we now conclude that the B_6^{2-} cluster, whether in the isolated state or as a part of the LiB_6^- cluster, is both σ- and π-antiaromatic.

The question now is why the doubly antiaromatic C_{2v} structure I of LiB_6^- is more stable (by 45.1 kcal/mol at the B3LYP/6-311+G* level) than the doubly aromatic C_{6v} structure VII (Fig. 2)? The MO pictures for the C_{6v} structure VII show that six MOs [HOMO-3, HOMO-4, HOMO-4′, HOMO-5, HOMO-5′, and HOMO-6, Fig. 3(c)] corresponding to six $2c-2e$ B–B peripheral bonds, one completely delocalized aromatic σ-MO (HOMO-1) and three aromatic π-MOs (HOMO, HOMO′, and HOMO-2). As discussed above, the C_{2v} structure I also has six MOs [Fig. 3(a)] corresponding to six $2c-2e$ B–B peripheral bonds, two delocalized π-MOs, and two delocalized σ-MOs. Thus, the difference between the two structures is one less occupied π-MO and one more occupied σ-MO in the global minimum C_{2v} structure relative to the C_{6v} structure. Our interpretation of this MO flip is that B atoms generate enough electrostatic potentials in the central area of the B_6 cycle to favor more occupation of the delocalized σ-MO compared to the π-MO. Another interpretation is that the $C_{2v}B_6^{2-}$ contains two highly stable and aromatic B_3^- units, as discussed next.

VIII. THE B_6^{2-} DIANION: FUSION OF TWO DOUBLY AROMATIC B_3^- UNITS

The doubly antiaromatic B_6^{2-} dianion can be viewed as the fusion of two B_3^- units. The B_3^- cluster was previously shown to be a highly stable, doubly (π- and σ-) aromatic species.[39] The MOs of the B_3^- species are shown in Fig. 3(d). The HOMO-1 ($1a_2''$) of B_3^- is a completely bonding π-orbital, formed by the overlap of the $2p_z$-atomic orbitals of the three boron atoms. Two electrons occupying this orbital satisfies the $4n+2$ Hückel's rule ($n=0$) for aromaticity. The HOMO ($2a_1'$) of B_3^- is a completely delocalized and bonding MO composed of the radial $2p$-AOs of the three boron atoms. Thus, B_3^- also satisfies the $4n+2$ Hückel's rule for σ-aromaticity, making it doubly aromatic.

We can interpret the global minimum B_6^{2-} (C_{2v}, $^1A_1$) dianion [Fig. 3(a)] in terms of two fused B_3^- species. The HOMO-9 ($1a_1$) and HOMO-8 ($1b_2$) of B_6^{2-} are really linear combinations (the sum and the difference) of the HOMO-3 ($1a_1'$) of two B_3^-. The HOMO-7 ($1b_1$) in B_6^{2-} is the sum of two HOMO-2 ($1e'$) of B_3^-. The bonding combination of two HOMO-2′ ($1e'$) in B_3^- gives rise to HOMO-6 ($2a_1$) in B_6^{2-}. The HOMO-4 in B_6^{2-} is simply the antibonding combination of two HOMO-2 ($1e'$) of B_3^-. The HOMO in B_6^{2-} is an antibonding combination of two HOMO-2′ of B_3^-. The π-bonding orbital HOMO-5 ($3a_1$) of B_6^{2-} is formed by the summation of two HOMO-1 ($1a_2''$) of B_3^-, and the HOMO-1 ($2b_2$) is an antibonding combination of these π-orbitals. The linear combination of HOMO ($2a_1'$) of two B_3^- gives the HOMO-3 ($4a_1$) (bonding combination) in B_6^{2-}. The HOMO-2 ($2b_1$) of B_6^{2-} is not formed by linear combination of occupied MOs of B_3^-. Instead it is the bonding combination of the LUMO ($2e'$) of B_3^-. Also, the antibonding combination of the two HOMOs of B_3^- is not occupied in B_6^{2-}. It should be pointed out that if all bonding and antibonding combinations of the occupied MOs in B_3^- are occupied in B_6^{2-}, the net bonding effect between the two B_3^- groups would be zero. Thus, the bonding between the two B_3^- units is due to the occupation of the bonding combination of the LUMOs in B_3^-, which happened to be bonding in the area between two B_3^- groups (the square part in B_6^{2-}), and due to unoccupation of the antibonding combination of HOMOs of B_3^-, which happened to be antibonding in the area between two B_3^- groups. We calculated the ΔE of dissociation of LiB_6^- into B_3^- and $Li^+B_3^-$ and found it to be 105.0 kcal/mol at the B3LYP/6-311+G* level of theory.

The MO analysis of LiB_6^- above showed that both π-bonding and antibonding combinations of the π-MOs in B_3^- are occupied in B_6^{2-}. Thus, π-MOs do not contribute to the chemical bonding between two B_3^- groups. That allows us to speculate that π-MOs could be considered as localized over two triangular areas in B_6^{2-}, i.e., island aromaticity. In

order to test this, we optimized the geometry for the neutral Li_2B_6 cluster. The $D_{2h}(^1A_g)$ structure, containing one Li^+ cation above and another Li^+ below the plane of the B_6^{2-} dianion, was found to be a saddle point on the potential energy surface. Geometry optimization, following the normal mode of the imaginary frequency, led to a $C_{2h}(^1A_1)$ structure with two Li^+ ions located above and below the two B_3^- triangular areas in B_6^{2-}. These results confirmed the presence of the π-island aromaticity in B_6^{2-}.

In contrast, the Al_6^{2-} cluster is known to have an octahedral structure in its global minimum form.[72] The planar D_{2h} isomer was found to be substantially higher in energy. It was shown that the lowest six MOs ($1a_{1g}$, $1a_{2u}$, $1e_u$, and $1e_g$) of Al_6^{2-} (Fig. 6 in Ref. 72) are simply sums and differences between the three lowest MOs ($1a'$ and $1e'$) of Al_3^- and thus they represent linear combinations of the six $3s^2$ lone pairs of Al. The next two MOs ($2a_{1g}$ and $3a_{1g}$) are sums of the delocalized σ ($2a_1'$) and π ($1a_2''$) MOs of Al_3^- and they are responsible for bonding interactions between two Al_3^- units as well as within these groups. Their corresponding antibonding combinations are empty, and instead, the bonding combination of $2e'$-LUMOs in Al_3^- is occupied. From this analysis it is clear that the preferred occupation of the bonding MOs derived from the $2e'$ LUMOs of Al_3^- causes the fusion of two Al_3^- into Al_6^{2-} and gives it structural stability. The planar D_{2h} isomer is substantially less stable, because Al_6^{2-} does not favor the presence of four π-electrons. The ability of boron clusters to favor the rather large number of π-electrons, on the other hand, gives rise to planar structures for B_6^{2-}. This is in contrast to aluminum clusters, which tend to reject large numbers of π-electrons and form three-dimensional structures.

IX. CONCLUSIONS

We produced a charge-transfer cluster, LiB_6^-, and characterized its electronic structure using by photoelectron spectroscopy. Extensive *ab initio* calculations revealed that LiB_6^- possesses a pyramidal singlet C_{2v} ground state structure, with a C_2 triplet isomer being a few kcal/mol higher in energy. Careful comparison between the photoelectron spectra and the *ab initio* one-electron detachment energies allows us to establish that the singlet C_{2v} structure is the ground state for the LiB_6^- anion. A detailed MO analysis is conducted for the D_{2h} B_6^{2-} and the C_{2v} LiB_6^-. The bare B_6^{2-} dianion, or in the $Li^+B_6^{2-}$ complex, is shown to be doubly (σ- and π-) antiaromatic and can be viewed as the fusion of two aromatic B_3^- units. In B_6^{2-}, the preferred occupation of the MO derived from the sums of the $2e'$ LUMO of B_3^-, rather than those derived from the differences between the $2a_1'$ HOMO of B_3^-, provides the critical bonding interactions in the planar B_6^{2-}.

ACKNOWLEDGMENTS

The theoretical work done at Utah was supported by the National Science Foundation (Grant No. CHE-0404937). The experimental work done at Washington was supported by the National Science Foundation (Grant No. DMR-0095828) and performed at the W. R. Wiley Environmental Molecular Sciences Laboratory, a national scientific user facility sponsored by Department of Energy (DOEs) Office of Biological and Environmental Research and located at Pacific Northwest National Laboratory, which is operated for DOE by Battelle.

[1] F. A. Cotton, G. Wilkinson, C. A. Murillo, and M. Bochmann, *Advanced Inorganic Chemistry*, 6th ed. (Wiley, New York, 1999).
[2] N. N. Greenwood and A. Earnshaw, *Chemistry of Elements*, 2nd ed. (Buttwerworth-Heinemann, Oxford, UK, 1997).
[3] A. C. Tang and Q. S. Li, Int. J. Quantum Chem. **29**, 579 (1986).
[4] L. Hanley, J. L. Whitten, and S. L. Anderson, J. Phys. Chem. **92**, 5803 (1988).
[5] R. Hernandez and J. Simons, J. Chem. Phys. **94**, 2961 (1991).
[6] A. U. Kato and E. Tanaka, J. Comput. Chem. **12**, 1097 (1991).
[7] A. U. Kato, K. Yamashita, and K. Morokuma, Chem. Phys. Lett. **190**, 361 (1990).
[8] J. M. L. Martin, J. P. Francois, and R. Gijbels, Chem. Phys. Lett. **189**, 529 (1992).
[9] R. Kawai and J. H. Weare, Chem. Phys. Lett. **191**, 311 (1992).
[10] A. K. Ray, I. A. Howard, and K. M. Kanal, Phys. Rev. B **45**, 14247 (1992).
[11] I. Boustani, Int. J. Quantum Chem. **52**, 1081 (1994).
[12] A. Meden, J. Mavri, M. Bele, and S. Pejovnik, J. Phys. Chem. **99**, 4252 (1995).
[13] I. Boustani, Chem. Phys. Lett. **233**, 273 (1995).
[14] I. Boustani, Chem. Phys. Lett. **240**, 135 (1995).
[15] I. Boustani, Surf. Sci. **370**, 355 (1996).
[16] A. Ricca and C. W. Bauschlicher, Chem. Phys. **208**, 233 (1996).
[17] A. Ricca and C. W. Bauschlicher, J. Chem. Phys. **106**, 2317 (1997).
[18] J. Niu, B. K. Rao, and P. Jena, J. Chem. Phys. **107**, 132 (1997).
[19] I. Boustani, Phys. Rev. B **55**, 16426 (1997).
[20] F. L. Gu, X. M. Yang, A. C. Tang, H. J. Jiao, and P. V. R. Schleyer, J. Comput. Chem. **19**, 203 (1998).
[21] I. Boustani and A. Quandt, Comput. Mater. Sci. **11**, 132 (1998).
[22] I. Boustani, A. Rubio, and J. A. Alonso, Chem. Phys. Lett. **311**, 21 (1999).
[23] M. L. McKee, Z. X. Wang, and P. V. R. Schleyer, J. Am. Chem. Soc. **122**, 4781 (2000).
[24] J. E. Fowler and J. M. Ugalde, J. Phys. Chem. A **104**, 397 (2000).
[25] J. Aihara, J. Phys. Chem. A **105**, 5486 (2001).
[26] Q. S. Li and H. W. Jin, J. Phys. Chem. A **106**, 7042 (2002).
[27] R. W. A. Havernith, P. W. Fowler, and E. Steiner, Chem.-Eur. J. **8**, 1068 (2002).
[28] S. Chacko, D. G. Kanhere, and I. Boustani, Phys. Rev. B **68**, 035414 (2003).
[29] J. Ma, Z. Li, K. Fan, and M. Zhou, Chem. Phys. Lett. **372**, 708 (2003).
[30] L. Hanley and S. L. Anderson, J. Phys. Chem. **91**, 5161 (1987).
[31] L. Hanley and S. L. Anderson, J. Chem. Phys. **89**, 2848 (1988).
[32] P. A. Hintz, S. A. Ruatta, and S. L. Anderson, J. Chem. Phys. **92**, 292 (1990).
[33] S. A. Ruatta, P. A. Hintz, and S. L. Anderson, J. Chem. Phys. **94**, 2833 (1991).
[34] P. A. Hintz, M. B. Sowa, S. A. Ruatta, and S. L. Anderson, J. Chem. Phys. **94**, 6446 (1991).
[35] S. J. La Placa, P. A. Roland, and J. J. Wynne, Chem. Phys. Lett. **190**, 163 (1992).
[36] M. B. Sowa-Resat, J. Smolanoff, A. Lapiki, and S. L. Anderson, J. Chem. Phys. **106**, 9511 (1997).
[37] S. J. Xu, J. M. Nilles, D. Radisic, W. J. Zheng, S. Stokes, K. H. Bowen, R. C. Becker, and I. Boustani, Chem. Phys. Lett. **379**, 282 (2003).
[38] M. Wyss, E. Riaplov, A. Batalov, J. P. Maier, T. Weber, W. Meyer, and P. Rosmus, J. Chem. Phys. **119**, 9703 (2003).
[39] H. J. Zhai, L. S. Wang, A. N. Alexandrova, A. I. Boldyrev, and V. G. Zakrzewski, J. Phys. Chem. A **107**, 9319 (2003).
[40] H. J. Zhai, L. S. Wang, A. N. Alexandrova, and A. I. Boldyrev, J. Chem. Phys. **117**, 7917 (2002).
[41] A. N. Alexandrova, A. I. Boldyrev, H. J. Zhai, L. S. Wang, E. Sheiner, and P. W. Fowler, J. Phys. Chem. A **107**, 1359 (2003).
[42] A. N. Alexandrova, A. I. Boldyrev, H. J. Zhai, and L. S. Wang, J. Phys. Chem. A **108**, 3509 (2004).
[43] H. J. Zhai, L. S. Wang, A. N. Alexandrova, and A. I. Boldyrev, Angew. Chem., Int. Ed. **42**, 6006 (2003).
[44] H. J. Zhai, B. Kiran, J. Li, and L. S. Wang, Nat. Mater. **2**, 827 (2003).

[45] A. E. Kuznetsov and A. I. Boldyrev, Struct. Chem. **13**, 141 (2002).
[46] A. N. Alexandrova, H. J. Zhai, L. S. Wang, and A. I. Boldyrev, Inorg. Chem. **43**, 3552 (2004).
[47] Q. S. Li and Q. Jin, J. Phys. Chem. A **107**, 7869 (2003).
[48] L. S. Wang, H. S. Cheng, and J. Fan, J. Chem. Phys. **102**, 9480 (1995).
[49] L. S. Wang and H. Wu, in *Advances in Metal and Semiconductor Clusters. IV. Cluster Materials*, edited by M. A. Duncan (JAI, Greenwich, 1998), p. 299.
[50] A. N. Alexandrova and A. I. Boldyrev (unpublished).
[51] A. N. Alexandrova, A. I. Boldyrev, Y.-J. Fu, X.-B. Wang, and L.-S. Wang, J. Chem. Phys. **121**, 5709 (2004).
[52] R. G. Parr and W. Yang, *Density-Functional Theory of Atoms and Molecules* (Oxford University Press, Oxford, 1989).
[53] A. D. Becke, J. Chem. Phys. **98**, 5648 (1993).
[54] J. P. Perdew, J. A. Chevary, S. H. Vosko, K. A. Jackson, M. R. Pederson, D. J. Singh, and C. Fiolhais, Phys. Rev. B **46**, 6671 (1992).
[55] M. J. Frisch, G. M. Trucks, H. B. Schlegel *et al.*, GAUSSIAN03 (revision A.1). (Gaussian, Inc., Pittsburgh, PA, 2003).
[56] D. M. Deaven and K. M. Ho, Phys. Rev. Lett. **75**, 288 (1995).
[57] R. Krishnan, J. S. Binkley, R. Seeger, and J. A. Pople, J. Chem. Phys. **72**, 650 (1980).
[58] J. Cizek, Adv. Chem. Phys. **14**, 35 (1969).
[59] P. J. Knowles, C. Hampel, and H.-J. Werner, J. Chem. Phys. **99**, 5219 (1993).
[60] T. Clark, J. Chandrasekhar, G. W. Spitznagel, and P. V. R. Schleyer, J. Comput. Chem. **4**, 294 (1983).
[61] M. J. Frisch, J. A. Pople, and J. S. Binkley, J. Chem. Phys. **80**, 3265 (1984).
[62] E. D. Glendening, A. E. Reed, J. E. Carpenter, and F. Weinhold, NPA Version 3.1.
[63] R. Bauernshmitt and R. Alrichs, Chem. Phys. Lett. **256**, 454 (1996).
[64] M. E. Casida, C. Jamorski, K. C. Casida, and D. R. Salahub, J. Chem. Phys. **108**, 4439 (1998).
[65] K. Raghavachari, G. W. Trucks, J. A. Pople, and M. Head-Gordon, Chem. Phys. Lett. **157**, 479 (1989).
[66] L. S. Cederbaum, J. Phys. B **8**, 290 (1975).
[67] V. G. Zakrzewski and W. J. von Niessen, Comput. Chem. (Oxford) **14**, 13 (1993).
[68] V. G. Zakrzewski and J. V. Ortiz, Int. J. Quantum Chem. **53**, 583 (1995).
[69] For a review see: J. V. Ortiz, V. G. Zakrzewski, and O. Dolgunitcheva, Conceptual Trends Quantum Chem. **3**, 463 (1997).
[70] M. J. Frisch, G. M. Trucks, H. B. Schlegel *et al.*, GAUSSIAN98 (revision A.7) (Gaussian, Inc., Pittsburgh, PA, 1998).
[71] G. Schaftenaar, MOLDEN3.4 (CAOS/CAMM Center, The Netherlands, 1998).
[72] A. E. Kuznetsov, A. I. Boldyrev, H. J. Zhai, X. Li, and L. S. Wang, J. Am. Chem. Soc. **124**, 11791 (2002).